International Journal of Research
Available at https://edupediapublications.org/journals
e-ISSN: 2348-6848
p-ISSN: 2348-795X
Volume 04 Issue 13
October 2017

Supression of Harmonics Resonance in a Distribution Power System with Resonant Current Control

*AKULA.ROJA **MR V SATYANARAYANA

*PG SCHOLAR,DEPARTMENT OF EEE, VAAGDEVI COLLEGE OF ENGINEERING(UGC-AUTONOMOUS, ACCREDITED BY NBA)

**ASSISTANT. PROFESSOR, DEPARTMENT OF EEE, VAAGDEVI COLLEGE OF ENGINEERING(UGC-AUTONOMOUS, ACCREDITED BY NBA)

ABSTARCT: Harmonic distortion is mainly due to the tuned passive filter and line inductance which produces resonances in the industrial system. To suppress this above problem hybrid active filter is used. The proposed hybrid filter is operated as variable conductance according to the total harmonic distortion in voltage and current. Thus harmonic distortion can be reduced to an acceptable level in the power system. The hybrid active filter is a combination of seventh tuned passive filter and an active filter in series connection so that the VA rating of the active filter and the dc voltage of the active filter are reduced to acceptable levels and in addition to that hybrid active filter is used because of its filtering capability and the cost. A Design consideration is presented and experimental results are provided to validate the effectiveness of the proposed method.

Keywords— Harmonic resonance, Hybrid active filter,

1. INTRODUCTION The extensive usage of nonlinear loads such as adjustable speed drives, uninterruptable power supply and battery charging system increases the harmonic pollution. The diodes or rectifiers are used to realize the power conversion because of lower component cost and its simplicity. Moreover rectifiers allow a large amount of harmonic current flow in the system. This excessive power flow produces harmonic distortion which may give rise to malfunction of sensitive equipment. Normally tuned passive filter are located at the secondary side of the distribution transformer to provide low impedance for controlling harmonic current and to correct the power factor for harmonic loads[1],[2].To provide the parametric changes in the passive filters, results in unintended series or parallel resonances that may occur between the passive filter and the line inductance. The functionality of passive filter may become progressively worse and extra calibrating work is needed to maintain the filtering capability.[3],[4]. Various active filtering technique have been presented to indicate the harmonic issues in the power system [5]-[7].The active filter is used for compensating harmonic currents of non-linear loads, butthis may not be effective.To improve the performance of the passive filter “active inductance” hybrid filter was introduced [10].The fifth harmonic resonance is present between the power system and the capacitor bank. In order to suppress that fifth harmonic resonance a hybrid shunt active filter with filter –current detecting capability was used. The combination of both the active and the passive filter in series with the capacitor bank by coupling a transformer was used to reduce the harmonic

resonance and to balance the harmonic current.[12],[13].This method needs extra transformers or tuned passive filter to maintain the filtering capability A transformerless hybrid active filter was presented to compensate harmonic current and or fundamental reactive current [14] –[19].A hybrid active filter with damping conductance was proposed to suppress harmonic voltage propagation in distribution power systems [20].The resonance between the passive filter and the inductance is not considered in the system. The fixed conductance may deteriorate the damping performances. An anti-resonance hybrid filter for delta-connected capacitor bank of power-factorcorrection applications is presented [21]. This in circuit was limited to three single-phase inverters, and the filtering performance was not considered. In addition, the hybrid active filter was proposed for the unified Power Quality (PQ) conditioner to address PQ issues in the power distribution system [22]. Several case studies of the hybrid active filter considering optimal voltage or current distortion were conducted

OPERATION PRINCIPLE

A simplified one-line circuit diagram of the proposed active filter and the associated control are shown in Fig.4.1. The active filter unit (AFU) is installed at the end of a radial line to suppress harmonic resonance. The AFU operates as a variable conductance for different harmonic frequency as given,

$$I^{*}_{abc,h} = \sum G_h^{*}.E_{abc,h} \quad (1)$$

where h represents the order of the harmonic frequency. The conductance command G∗ h is defined as a control gain to dampen harmonic voltage Eabc,h. As shown in Fig.5.1, the control is composed of harmonic-voltage extraction and tuning control, followed by the current regulation and PWM algorithm. Operation principle and design consideration are given as follows.

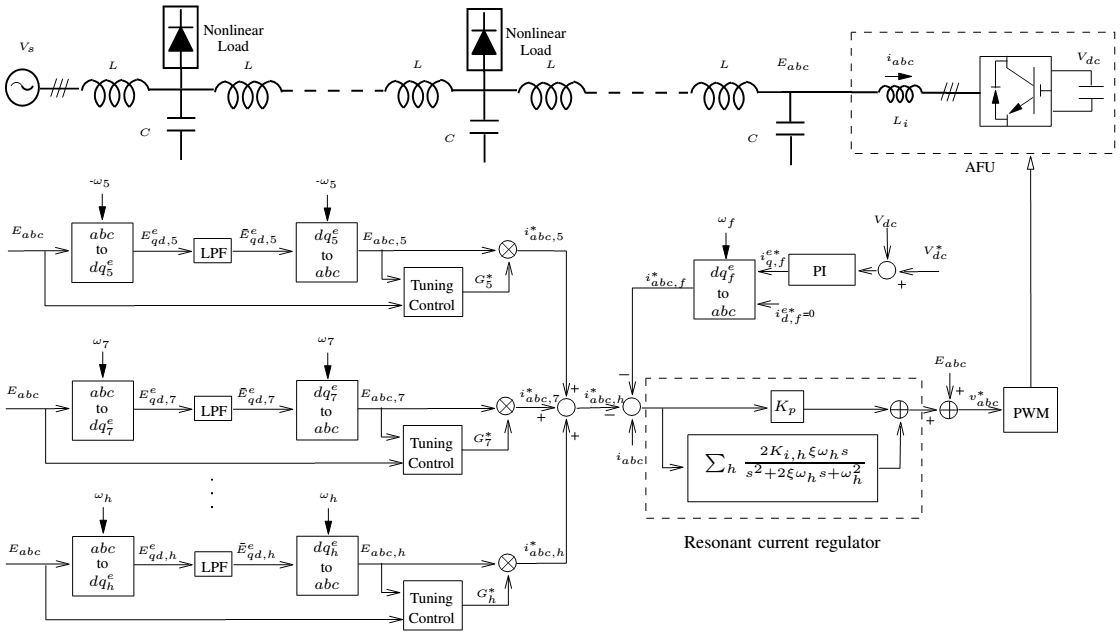

Fig. 4.1. Active filter and the associated control.

AFU control

Harmonic voltage at the different frequency is determined based on the so-called synchronous reference frame (SRF) transformation. The specific harmonic voltage component becomes a dc value after Eabc is transformed into the SRF at ωh, Accordingly, a low-pass filter (LPF) is applied to separate the dc value and then the corresponding harmonic component E abc,h is obtained when applying reverse transformation. It is worth noting here that a phase-locked loop (PLL) is required to determine system frequency for implementation of SRF. ωh should be set as a negative value for negative-sequence component (i.e., fifth) or a positive value for positive-sequence harmonic component (i.e., seventh), respectively.

Fig.4.2 shows the tuning control for the conductance command G∗ h. As illustrated, G∗h is determined according to the harmonic voltage distortion VDh at the AFU installation point Eabc, in which VDh is defined as the percentage ratio of the harmonic voltage component Eh (rms value) to the voltage E (rms value) by

$$VD_h = \frac{E_{h,RMS}}{E_{RMS}}.100\%$$

$$E_{h,RMS} = \sqrt{\frac{\int_t^{t+T}(E_{a,h}(t)^2+E_{b,h}(t)^2+E_{c,h}(t)^2)}{T}dt} \qquad (2)$$

$$E_{RMS} = \sqrt{\frac{\int_t^{t+T}(E_{a,h}(t)^2 + E_{b,h}(t)^2 + E_c\,(t)^2)}{T}dt}$$

The derivation of VDh is approximately evaluated by using two LPFs with cut-off frequency at ωc, which are to filter out ripple components in the calculation. The error between the allowable harmonic voltage distortion VD∗h and the actual harmonic voltage distortion VDh is then fed into a proportional lintegral (PI) regulator to adjust the conductance command G∗h. Hence, a variable conductance command G∗h for the different harmonic frequency is generated.

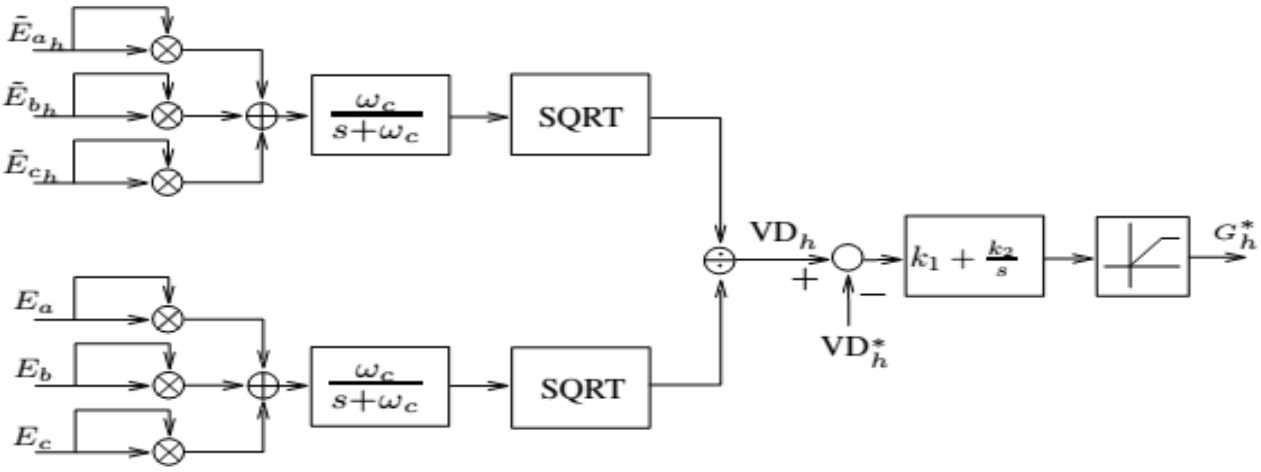

Fig4.2 Tuning control of the conductance command.

The total current command is the summation of fundamental current command $i^*_{abc,f}$ and all harmonic current commands $i^*_{abc,h}$, which is equal to the product of the harmonic voltage and its corresponding conductance command. $i^*_{abc,f}$ shown in Fig.4.1 is the in-phase fundamental current command generated by a PI control to control the dc voltage Vdc of the AFU. In order for the active filter to guarantee current tracking capability, the resonant current regulator is realized by:

$$T_r(S) = k_p + T_r(s) = k_p + \sum_h \frac{2k_{i,h}\xi w_h s}{s^2+2\xi w_h s+w_h^2} \qquad (3)$$

where k p is a proportional gain and ki,h is an integral gain for individual harmonic frequency, respectively. The current control is tuned to resonate at harmonic frequencies ωh, so that various narrow gain peaks centered at harmonic frequencies are introduced. The damping ratio ξ is designed to determine the selectivity and bandwidth of the current control. Accordingly, the voltage command vabc∗ is obtained for PWM to synthesize the output voltage of the active filter.

4.2 Modelling of control

Nomenclature used in this section is given as:

Vsh(s): harmonic voltage at the source terminal

Eh(s): harmonic voltage at the installation location of the active filter

Ih(s) : harmonic current of the active filter

I∗ h(s) : harmonic current command of the active filter

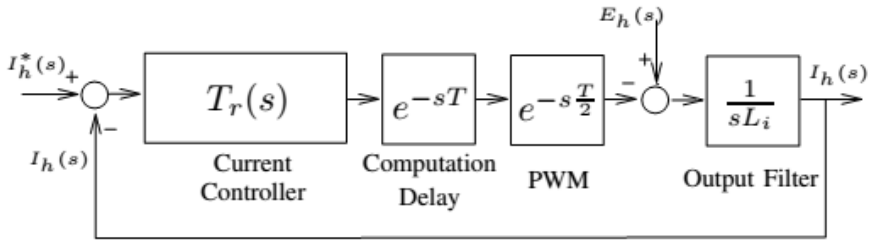

Fig5.3 Current control block diagram of the proposed AFU.

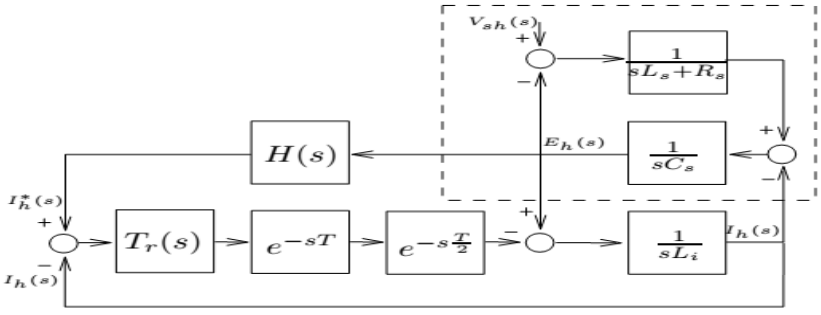

Fig4. 4. Voltage control block diagram of the proposed AFU in the distributed power system.

Fig.4.3 shows current control block diagram for each phase. Digital signal processing delay and PWM delay are included, where T represents a sampling period. Hence, current loop stability and current tracking capability can be simply evaluated by using bode plots of open-loop and closed-loop transfer functions. Fig.4.4 shows the block diagram for harmonic damping analysis. Since high-order harmonics seldom excite resonances, the distribution network is replaced with a second order resonant tank (Ls, Cs, Rs) as indicated by the dashed box. Here, the resonant tank is tuned to amplify the harmonic voltage Eh(s). Note that the scheme of harmonic detection at ωh is equivalent to a single-side band pass filter in the stationary frame. The transfer function H(s) can be expressed as (4), where ωh is the harmonic frequency and TLP F is time constant of the low-pass filter, which is used to filter out the dc component in the rotational reference frames. Thus the damping performance of the AFU can be evaluated by the harmonic-voltage magnification $\frac{|Eh(s)|}{|Vsh(s)|}$ shown in Fig.4.4.

$$H(s) = G_h^* \frac{(s-jw_h)T_{LPF}}{1+(S-jw_h)T_{LPF}} \qquad (4)$$

Table 1

Parameters of a given power line

Line voltage	11.4kV
Line frequency	60 Hz
Feeder length	9 km
Line inductor	1.55 mH / km(4.5%)
Line resister	0.36Ω/km(1.2%)
Line capacitor	22.7μF/km(11.1%)
Characteristic impedance,Z_0	8.45Ω
Wave length of 5^{th} harmonics	17.8 km
Wave length of 7_{th} harmonics	12.7 km

3Ø 11.4kV 10MVA base

4.3 Harmonic Resonance

In this section, the line distributed-parameter model is applied to evaluate harmonic resonance along the feeder. A sample feeder given in TABLE I can amplify harmonic voltage if harmonic standing wave is generated. The active filter is assumed to be installed at the end of the line (x = 9) with equivalent harmonic admittance Yh given in (5), where θh represents the lagging angle.

$$Y_h = |{}_hY| < \Theta_h. \qquad (5)$$

The voltage magnifying factor Mh(x) in (6) represents harmonic amplification along the feeder.

$$M_h(x) = \frac{|V_H(x)|}{|V_{s,h}|} \qquad (6)$$

The suffix h denotes the order of harmonics, vh(x) is the harmonic voltage at position x($0 \le x \le 9$), and vs,h is the harmonic voltage source (vs,h=vh(0)). Note that Mh(x) can be formulated by using standing wave equations considering both feeder and damping impedance provided by the filter.

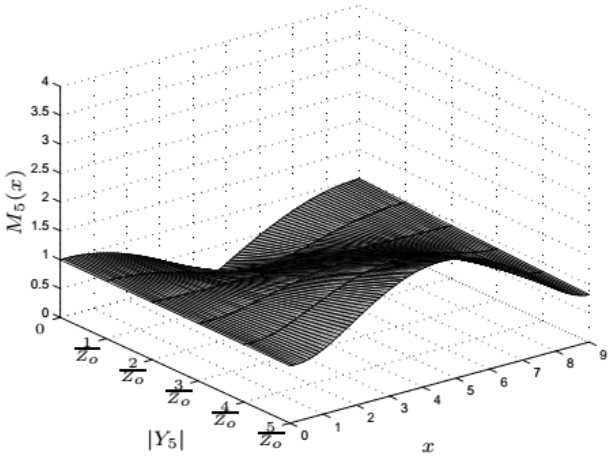

4.5(a) The magnifying factor of the fifth harmonic.

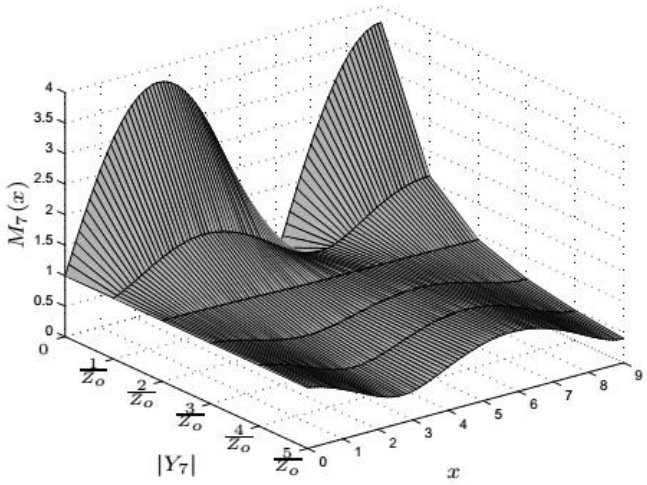

4.5(b) The magnifying factor of the seventh harmonic.

Fig. 4.5 The magnifying factor along the radial line if the active filter is modelled as |Y| with θ = 0o.

Harmonic conductance

Fig. 4.5 shows Mh along the line when the active filter is modelled as a purely harmonic conductance, i.e. θh=0. M5 shows no amplification in case of no active filtering (|Yh|=0). However, M7 is strongly amplified due to seventh harmonic resonance as shown in Fig.5.5(b). This results from the standing wave of seventh harmonics (3/4λ7 ≈ 8 km). On the contrary, M5 on the middle segment of the line is increased with increasing |Yh|. Fig. 4.5(a) shows M5 is unintentionally amplified if the active filter is operated in overdamping condition(|Yh| > Zo−1). This phenomenon is due to fifth harmonic resonance (λ5/2 ≈ 8 km), which is referred as the ”whack-a-mole”. Note that both M5 and M7 can be suppressed at the same time only when the active filter is operated at the perfect matching condition, i.e. |Yh|=Zo−1.

Harmonic admittance

Fig.4.6 and Fig.4.7 show M5 and M7 when the active filter is modelled as harmonic admittance |Yh| with θ = −45o and θ = −90o, respectively.

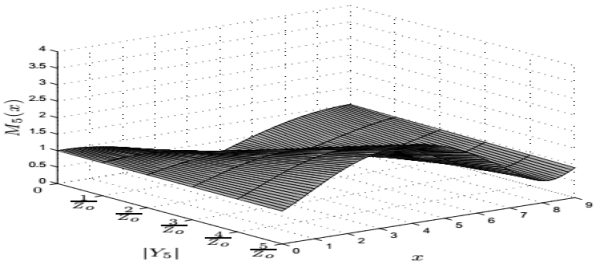

4.6(a)The magnifying factor of the fifth harmonic for.

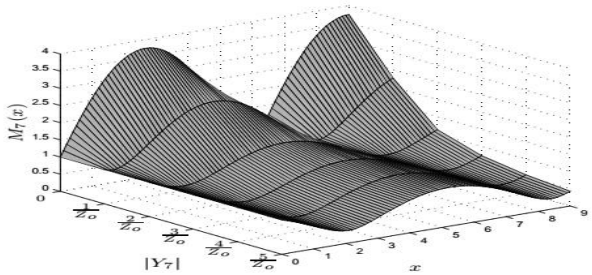

4.6(b) The magnifying factor of the seventh harmonic.

Fig4.6. The magnifying factor along the radial line if the active filter is modelled as |Y| with θ = −45o

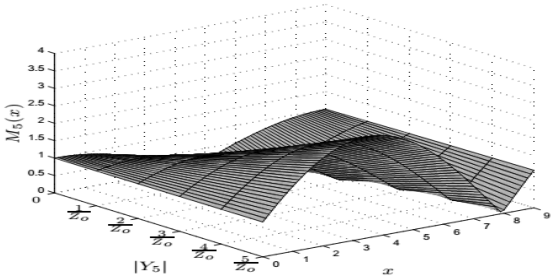

4.7(a) The magnifying factor of the fifth harmonic.

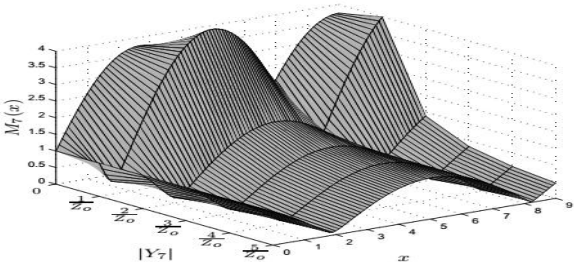

4.7(b) The magnifying factor of the seventh harmonic.

Fig4.7 The magnifying factor along the radial line if the active filter is modelled as |Y| with θ = −90o.

As observed, increasing |Yh| can enhance the damping capability at the end of the line only, but may result in the ”whack-a-mole” issue. Harmonic voltage is not able to be effectively mitigated even when the active filter is in operation. Fig.5.7 shows voltage distortion near the middle segment of the line becomes much more significant in case of θ = −90o. Therefore, the active filter operating as harmonic

admittance may not effectively suppress harmonic resonances, or even induce other harmonic resonances at other locations on the feeder. The active filter should be controlled as purely harmonic conductance to ensure harmonic damping capability in the distribution power system.

SIMULATION STUDIES

In order to demonstrate harmonic damping performance, the active filter with the proposed control is simulated by using the alternative transient program (ATP). Note that high order harmonics (>7) seldom excite obvious resonances in the distribution system, so the resonant current control includes fifth and seventh resonant terms only.

• Power system: 3φ, 220 V(line-to-line), 20 kVA, 60 Hz. Base values are listed in TABLE II.

• Line parameters: L=3.1 %, C=13.7 %.

• Nonlinear loads: NL1 and NL2 are constructed by three phase diode-bridge rectifiers, and consume real power 0.25 pu, respectively.

• Linear loads: Both linear loads are initially off. LL1, LL2 are rated at 0.1 pu(pf=1.0), 0.09 pu(pf=0.9), respectively.

• Current control: k p=25, ki,5=100, ki,7=100, ξ=0.01.

• Tuning control: k1=100, k2=2000, ωc=62.8Rad/s, VD∗ h=3.0%.

• The AFU is implemented by a three-phase voltage source inverter with PWM frequency 10 kHz.

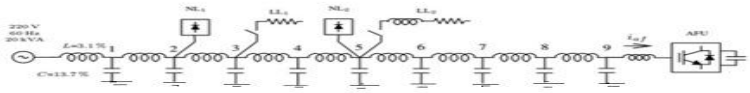

5.1(a) Simulation circuit configuration

Control Diagram

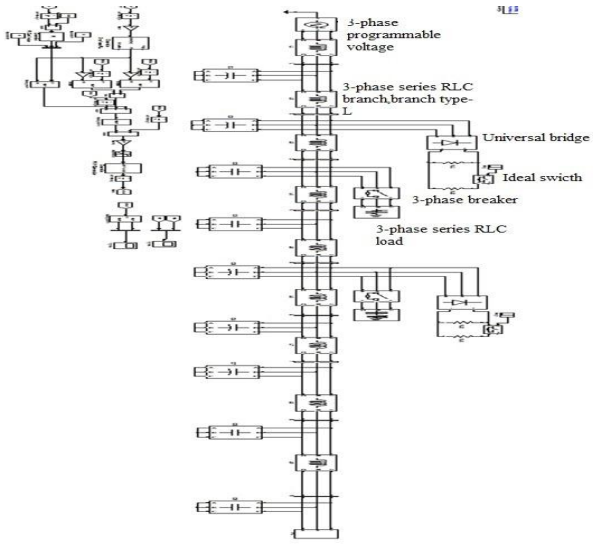

Fig 5.1(b) control diagram of AFU is on

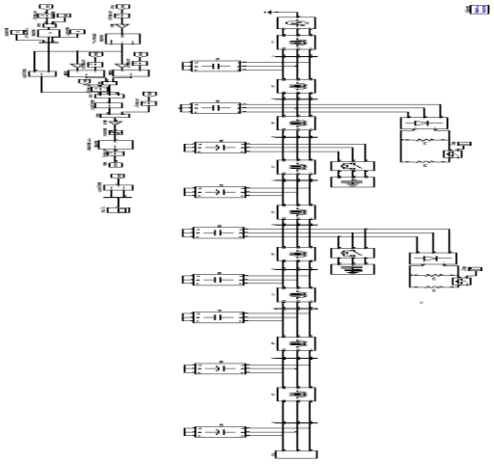

Fi5.1(c)control diagram of AFU off

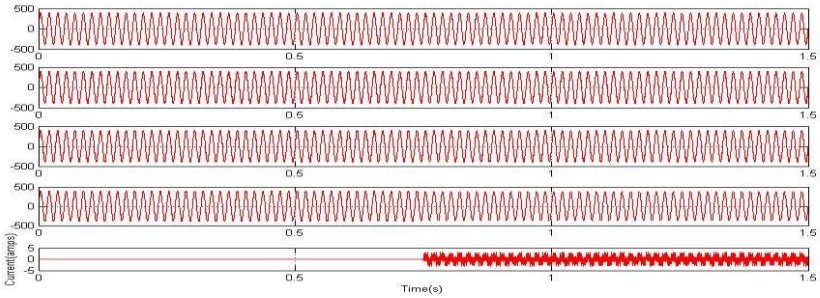

Fig5.1(d)AFU is on

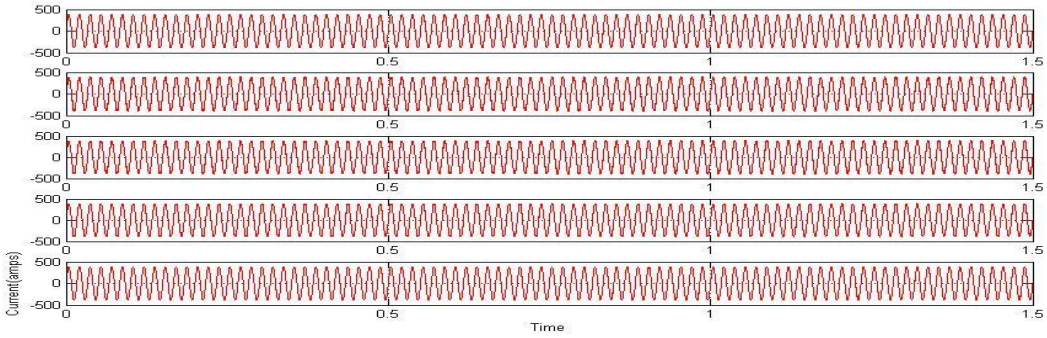

5.1(e) AFU is off

Fig5.1 Simulation circuit and steady-state results.

Steady-state results

Fig6.1(e) shows bus voltages are severely distorted before the AFU is initiated. For example, voltage THDs at bus 3 and bus 9 are 5.6% and 6.1%, respectively. Fig6.2 illustrates voltage distortion VD5, VD7 on each bus. We can observe that voltage

Table 2

Base Values

Voltage base	220V
Current base	52.5A
Impedance base	2.42Ω
Conductance base	$0.413\Omega^{-1}$

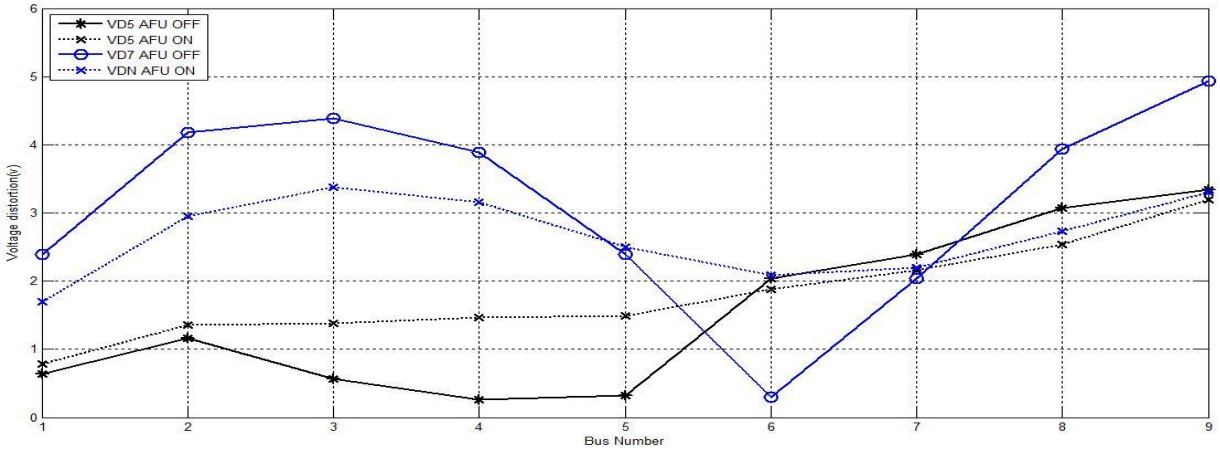

Fig5.2 VD5 and VD7 on all buses before and after the AFU is in operation.

distortion along the line is cyclically amplified and seven harmonic resonance is dominant. This result confirms the previous analysis by harmonic distributed-parameter model. After the AFU starts in operation, Fig5.1(d) shows voltage distortion is clearly improved. Voltage THD at bus 9 is reduced from 6.1 % to 4.4%, which contains 3.0% fifth harmonics and 3.0% seventh harmonics. The blue curves of Fig.5.2 demonstrates that both VD5 and VD7 become more uniform along the line. At the steady state, the AFU is operated at G∗5 = 1.14 pu and G∗ 7 = 1.28 pu with rms current 0.06 pu. Note that the voltage THD values at buses 5 and 6 are slightly increased from 2.9% to 3.3% and 2.9% to 3.6%, respectively. This result does not contradict the functionality of the active filter because the entire feeder shows more uniform voltage quality after damping.

Transient behavior

In this section, we evaluate transient behavior of the AFU. Nonlinear loads NL1, NL2 are first increased from 0.25 pu to 0.35 pu at t=1.5 s, t=2.0 s, respectively, and linear loads LL1, LL2 are subsequently turned on at t=2.5 s, t=3.0 s, respectively. Fig. 5.3(a) shows transient responses of voltage distortion when the AFU is off. Since increasing nonlinear loads results in high voltage distortion at t=1.5 s, t=2.0 s, respectively, Fig. 5.3(b) shows that the PI regulator of the tuning control raises both G∗5 and G∗7 commands to draw more harmonic current to reduce voltage distortion. On the contrary, linear loads can help reduce distortion. Accordingly, G∗5 and G∗ 7 are decreased at t=2.5 s, t=3.0 s, respectively. Fig. 5.3(c)

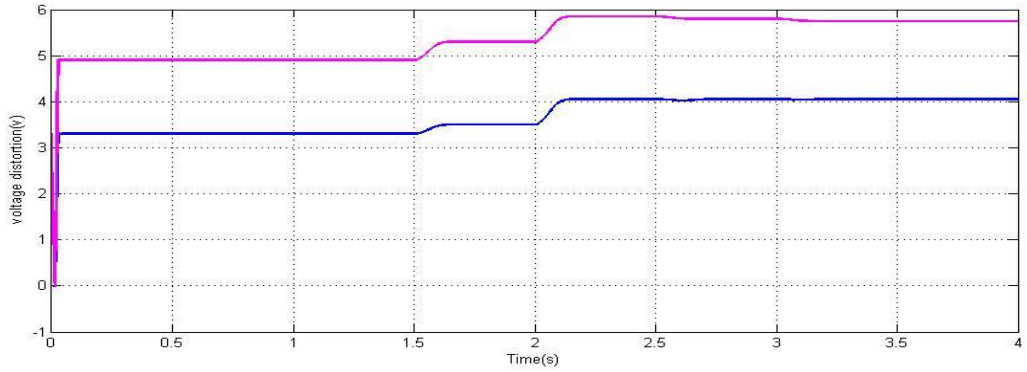

Fig5.3(a) Harmonic voltage distortion when the AFU is off.

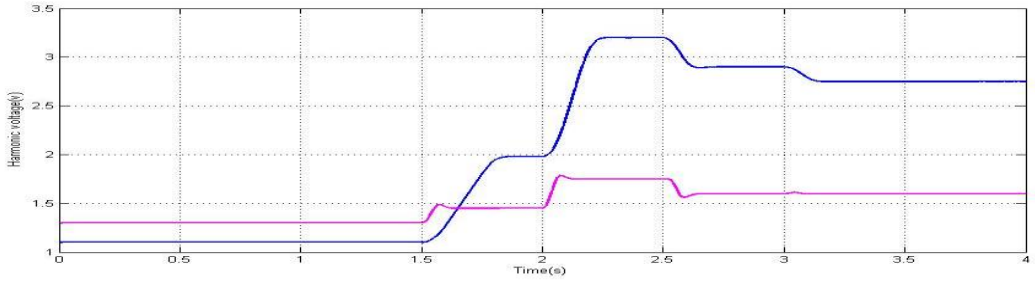

Fig 5.3(b) Active filter conductance commands

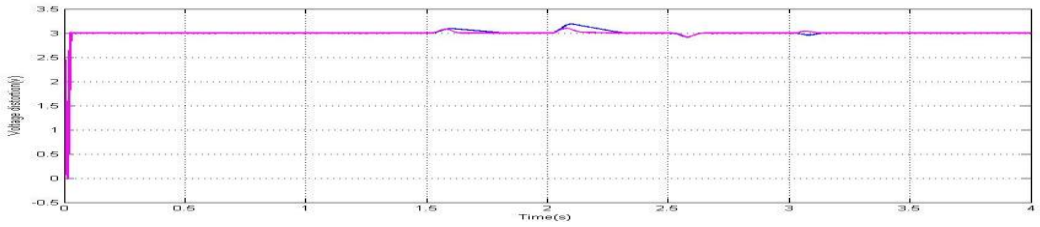

Fig5.3(c) Harmonic voltage distortion when the AFU is on.

Fig5.3 AFU transient behavior (NL1, NL2 are increased at t=1.5 s, t=2.0 s, respectively, and then LL1, LL2 are turned on at t=2.5 s, t=3.0 s, respectively.)

shows VD5, VD7 can be clearly maintained at 3% after short transient. It is worth nothing here that the overshoot of voltage distortion results from 0.1 pu load change in a stepped manner. This phenomenon could be avoided by tuning PI parameters (k1, k2). However, it may not cause practical issue because harmonic variation is usually slow in the distribution power system.

Current-loop analysis

In addition to the resonant current control (kp=25, ki=100), the proportional current control with k p=25, 50, and 100 are encompassed for comparative purpose. In there are magnitude peaks at both fifth and seventh harmonic frequencies as well as phase-leading compensation for the resonant current control. Therefore, the AFU is able to

function as an approximately pure conductance at fifth and seventh harmonic frequencies. In case of the proportional control with critically damped gain (kp=25), phase-lagging is so large that the AFU is actually operated as harmonic admittance. Increasing proportional gain is able to enhance current tracking performance, but the stability margin of the AFU may reduce. For example, the system is run at low stability margin in case of kp=50, or even the system becomes unstable for k p=100. That means system stability is very sensitive to the proportional gain. The resonant current control with complex poles (kp=25, ki=100) should be a better choice based on stability reason.

voltage THDs of time-domain simulations on all buses for different current control. The AFU with proportional control kp=25 is simply able to reduce voltage distortion at the installation location by significantly increasing fifth harmonic conductance command G∗5. However, the ”whack-a-mole” effect is induced so as to inversely amplify harmonic voltage on the middle segment of the line. In case of k p=50, damping performance becomes better but stability is a concerned issue. Obviously, the resonant current control provides best performance. TABLE III summarizes conductance commands and AFU currents. As can be seen, the AFU with the proportional control consumes larger current, but damping performances is not guaranteed. The AFU with the resonant current control is able to effectively damp harmonic resonance throughout the feeder at lower AFU current.

Table 3

Test Results For Different Current Controls

	G_5	G_7	RMS current
K_P=50	1.89pu	1.04pu	7.8%
K_P=25	3.39pu	0.90pu	12%
K_P=25,K_I=100	1.14pu	1.28pu	6%

Voltage damping analysis

In this section, harmonic suppression capability of the AFU is evaluated based on Fig.5.4 considering AFU control, including phase lagging and current control. The resonant tank(Cs=717uF, Ls=200uH, Rs=0.1) is tuned to amply seventh harmonic voltage. Fig.5.4(c)shows that seventh harmonic voltage is reduced and controlled by harmonic conductance after the AFU is turned on. This test can verify AFU effective Frequency characteristics of harmonic amplification.

6 Nonlinear loads at different locations

In this section, the damping performance of the AFU is evaluated when nonlinear loads are connected to different locations. Demonstrate voltage distortion on all buses when nonlinear loads at bus 2,5 , bus 3,7 , bus 4,6 , respectively. TABLE IV lists the corresponding G∗5 and G∗ 7, respectively. As shown, VD7 can be suppressed for all cases after the AFU is on. However, VD5 may increase in the middle segment of the line with increasing G∗5.Both VD5 and VD7 can be well suppressed when nonlinear loads are at bus 2,5. When nonlinear loads are changed to bus 3,7 Fig 5.5(a) the damping performance is not clear due to slight distortion. In case of nonlinear loads at bus 4,6, large fifth harmonic conductance (G∗5=3.15 pu) is required to reduce fifth voltage distortion. This results in serious fifth harmonic resonance. Therefore, the termination-

installation active filter may unintentionally induce fifth harmonic resonance due to the ”whack-a-mole” issue if large G∗5 is adopted. This problem might be resolved by using multiple active filters, for example distributed active filter systems .

Table 4

AFU Conductance Commands

	G^*_5	G^*_7
NL_s at Bus 2,5	1.14pu	1.28pu
NL_s at Bus 3,7	1.19pu	0.32pu
NL_s at Bus 4,6	3.15pu	1.23pu

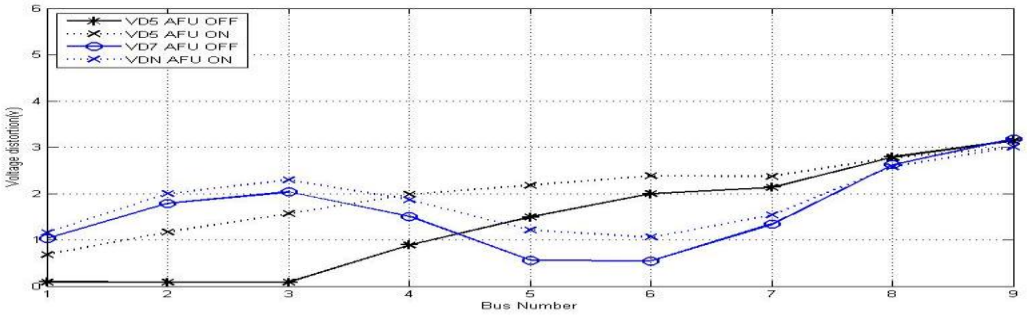

Fig5.5(a) Nonlinear loads are at bus 3 and bus 7.

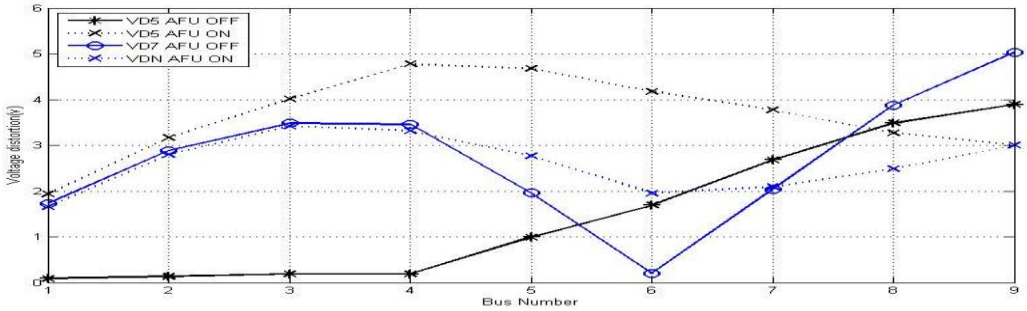

Fig5.5(b) Nonlinear loads are at bus 4 and bus 6.

Fig5.5 Harmonic damping performances when nonlinear loads are connected to different buses.

CONCLUSION

The active filter with the resonant current control is proposed in this project to suppress harmonic resonances in the distribution power system. The current control is implemented by various parallel band-pass filters tuned at harmonic frequencies so that the active filter can operate as an approximately pure harmonic conductance. A separate and tuning

conductance for different harmonic frequency is also realized to maintain the damping performance in response to load change or system variation. The contributions of this paper are summarized as follows. • Due to controlling delay, the damping active filter may unintentionally induce harmonic resonance at other locations in the feeder. This phenomenon is analyzed by using harmonic distributed-parameter model.

• Based on both simulations and experiments, the resonant current control is able to suppress harmonic resonance effectively.

• Both current loop and voltage loop are modeled to illustrate current-tracking capability and damping performance of the active filter.

• Damping performance of the active filter is discussed when nonlinear loads are located at different buses. Multiple active filters might provide more effective performance compared to the termination-installation one.

REFERENCES

[1] W. K. Chang, W. M. Grady, and M. J. Samotyj, "Meeting IEEE-519 harmonic voltage and voltage distortion constraints with an active power line conditioner," IEEE Trans. Power Del., vol. 9, no. 3, pp. 1531-1537, Jul. 1994.

[2] E. J. Currence, J. E. Plizga, and H. N. Nelson, "Harmonic resonance at a medium-sized industrial plant," IEEE Trans. Ind. Appl., vol. 31, no. 3, pp. 682-690, May/Jun. 1995.

[3] H. Akagi, "Control strategy and site selection of a shunt active filter for damping of harmonic propagation in power distribution system," IEEE Trans. Power Del., vol. 12, no. 2, pp. 354-363, Jan. 1997.

[4] C.-H. Hu, C.-J. Wu, S.-S. Yen, Y.-W. Chen, B.-A. Wu, and J.-S. Hwang, "Survey of harmonic voltage and current at distribution substation in northern taiwan," IEEE Trans. Power Del., vol. 12, no. 3, pp. 354-363, July 1997.

[5] Y. D. Lee, C. S. Chen, C. T. Hsu, and H. S. Cheng, "Harmonic analysis for

distribution system with dispersed generation systems," in International Conference on Power System Technology, 2006, pp. 1-6.

[6] V. Corasaniti, M. Barbieri, P. Arnera, and M. Valla, "Reactive and harmonics compensation in a medium voltage distribution network with active filters," in IEEE/ISIE International Symposium on Industrial Electronics, 2007, pp. 916-921.

[7] J. H. R. Enslin and P. J. M. Heskes, "Harmonic interaction between a large number of distributed power inverters and the distribution network," IEEE Trans. Power Electron., vol. 19, no. 6, pp. 1586-1593, Nov. 2004.

[8] IEEE Recommended practices and requirements for harmonic control in electrical power systems, IEEE Std. 519-1992, 1993.

[9] H. Akagi, H. Fujita, and K. Wada, "A shunt active filter based on voltage detection for harmonic termination of a radial power distribution line," IEEE Trans. Ind. Appl., pp. 638-645, May/Jun. 1999.

[10] K. Wada, H. Fujita, and H. Akagi, "Considerations of a shunt active filter based on voltage detection for installation on a long distribution feeder," IEEE Trans. Ind. Appl., pp. 1123-1130, Jul./Aug. 2002.

[11] P. Jintakosonwit, H. Fujita, H. Akagi, and S. Ogasawara, "Implementation and performance of cooperative control of shunt active filters for harmonic damping throughout a power distribution system," IEEE Trans. Ind. Appl., vol. 39, no. 2, pp. 556-564, Mar./Apr. 2003.

[12] M. Saito, T. Takeshita, and N. Matsui, "Modeling and harmonic suppression for power distribution system," IEEE Trans. Ind. Electron., vol. 50, no. 6, pp. 1148-1158, Dec. 2003.

[13] P.-T. Cheng and T.-L. Lee, "Distributed active filter systems (DAFSs): A new approach to power system harmonics," IEEE Trans. Ind. Appl., vol. 42, no. 5, pp. 1301-1309, Sept./Oct. 2006.

[14] W. K. Chang and W. M. Grady, "Minimizing harmonic voltage distortion with multiple current-constrained active power

line conditioners," IEEE Trans. Power Del., vol. 12, no. 2, pp. 837-843, Apr. 1997.

[15] K. Kennedy, G. Lightbody, R. Yacamini, M. Murray, and J. Kennedy, "Development of a network-wide harmonic control scheme using an active filter," IEEE Trans. Power Del., vol. 22, no. 3, pp. 1847-1856, Jul. 2007.

[16] I. Ziari and A. Jalilian, "A new approach for allocation and sizing of multiple active power-line conditioners," IEEE Trans. Power Del., vol. 25, no. 2, pp. 1026-1035, Apr. 2010

[17] X. Sun, J. Zeng, and Z. Chen, "Site selection strategy of single frequency tuned r-apf for background harmonic voltage damping in power systems," IEEE Trans. Power Electron., vol. 28, no. 1, pp. 135-143, Jan. 2013.

[18] P. Jintakosonwit, H. Fujita, and H. Akagi, "Control and performance of a full-digital-controlled shunt active filter for installation on a power distribution system," IEEE Trans. Power Electron., vol. 17, no. 1, pp. 132-140, Jan. 2002.

[19] D. M. Brod and D. W. Novotny, "Current control of vsi-pwm inverters," IEEE Trans. Ind. Appl., vol. 21, no. 4, pp. 562-570, Jun. 1985.

[20] P. Mattavelli and F. P. Marafao, "Repetitive-based control for selective harmonic compensation in active power filters," IEEE Trans. Ind. Electron., vol. 51, no. 5, pp. 1018-1024, Oct. 2004.

[21] T. G. Habetler, "A space vector-based rectifier regulator for AC/DC/AC converters," IEEE Trans. Power Electron., vol. 8, no. 1, pp. 30-36, Jan. 1993.

[22] T.-L. Lee, J.-C. Li, and P.-T. Cheng, "Discrete frequency tuning active filter for power system harmonics," IEEE Trans. Power Electron., vol. 24, no. 5, pp. 1209-1217, May 2009.

[23] L. Asiminoaei, F. Blaabjerg, and S. Hansen, "Detection is key - harmonic detection methods for active power filter applications," IEEE Ind. Appl. Mag., vol. 13, no. 4, pp. 22-33, July/Aug. 2007.

[24] C. Lascu, L. Asiminoaei, and F. Blaabjerg, "High performance current

controller for selective harmonic compensation in active power filters," IEEE Trans. Power Electron., vol. 22, no. 5, pp. 1826-1835, Sep. 2007.

[25] C. Lascu, L. Asiminoaei, I. Boldea, and F.Blaabjerg, "Frequency response analysis of current controllers for selective harmonic compensation in active power filters," IEEE Trans. Ind. Electron., vol. 56, no. 2, pp. 337-347, Feb. 2009.